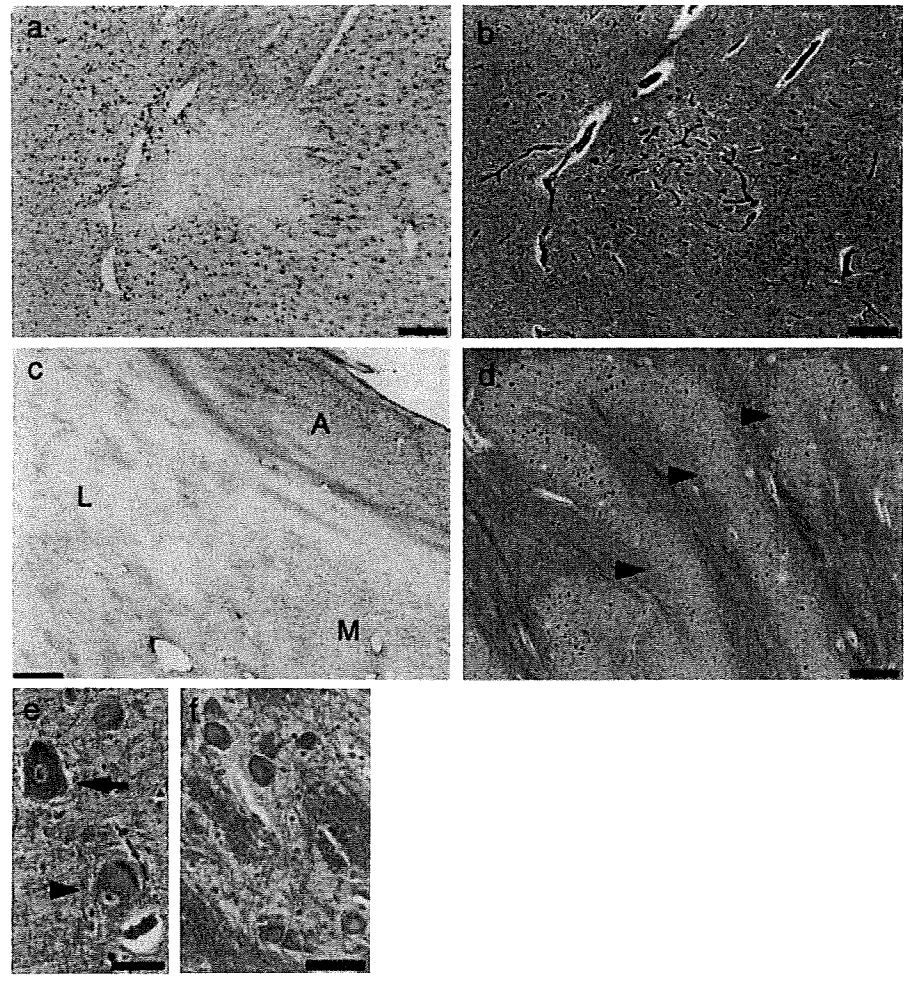

Fig. 3 (a) and (b) are serial sections. (a,b) Central necrosis with astrocytosis (a) and capillary proliferation (b) in the left inferior colliculi. Bar = 200 μm. (c) Astrocytosis in the mediodorsal nucleus (indicated with M) and anterior nucleus (indicated with A) of the right thalamus, with sparing of the lateral nucleus (indicated with L). Bar = 500 μm. (d) Patchy neuronal loss in the right inferior olivary nucleus (arrowhead). Bar = 200 μm. (e) Central chromatolysis of the Betz cell (arrowhead) and a normal Betz cell (arrow). Bar = 50 μm. (f) Central chromatolysis of the neurons in the pontine nucleus. Bar = 50 μm. (a, c) GFAP stain, (b) Reticulin silver stain, (d–f) KB stain.

along the aqueduct and fourth ventricle.[9,10] In the thalamus and inferior olivary nucleus, by contrast, neuronal loss is demonstrated with sparing of the neuropil and capillaries.[9] The distribution of lesions is associated with abundant thiamine-related glucose and oxygen metabolism.[11] Most surgical procedures that include gastrectomy, gastrojejunostomy, colectomy, gastric bypass surgery are risk factors for the development of Wernicke's encephalopathy.[8]

Various CNS disorders are seen in patients with Wernicke's encephalopathy. They include Marchiafava-Bignami disease,[6] pellagra encephalopathy,[12] and Morel's laminar sclerosis.[5] To date, pathomechanisms of Marchiafava-Bignami disease or Morel's laminar sclerosis have not been fully understood, although direct intoxication of alcohol or thiamine deficiency is considered to cause these diseases, while pellagra is thought to be caused by niacin deficiency.

Pellagra is classically characterized by a triad of dermatitis, diarrhea and dementia (or derilium), but dermatitis and diarrhea are often lacking.[13] Coexistence of Wernicke's encephalopathy or Marchiafava-Bignami disease makes the diagnosis of pellagra difficult. Based on the alcoholic background, thiamine therapy is started in most patients, but niacin is rarely started. Furthermore, antagonism between thiamine and niacin had also been suggested. The metabolic demands from a relative excess of thiamine may increase the requirements for pyridine coenzymes, nicotinamide adenine dinucleotide (NAD) and nicotinamide adenine dinucleotide phosphate (NADP). These require niacin as a cofactor. Serudaru *et al.* reported a case of a "late-onset" pellagra encephalopathy in an alcoholic patient who deteriorated after thiamine therapy.[13] This case and our case suggested that multiple vitamin therapy should be started when treating undiagnosed encephalopathies in patients with chronic alcoholism.

Pellagra encephalopathy presents with various symptoms such as dementia (or derilium), hypertonus, and myoclonus.[13] Serudaru *et al.* reported that hypertonus and myoclonus were associated with lesions of pontine nucleus and cerebellar dentate nucleus, respectively,[13] but correlation between the symptoms and brain lesions has not been fully established. Histopathologically, pellagra

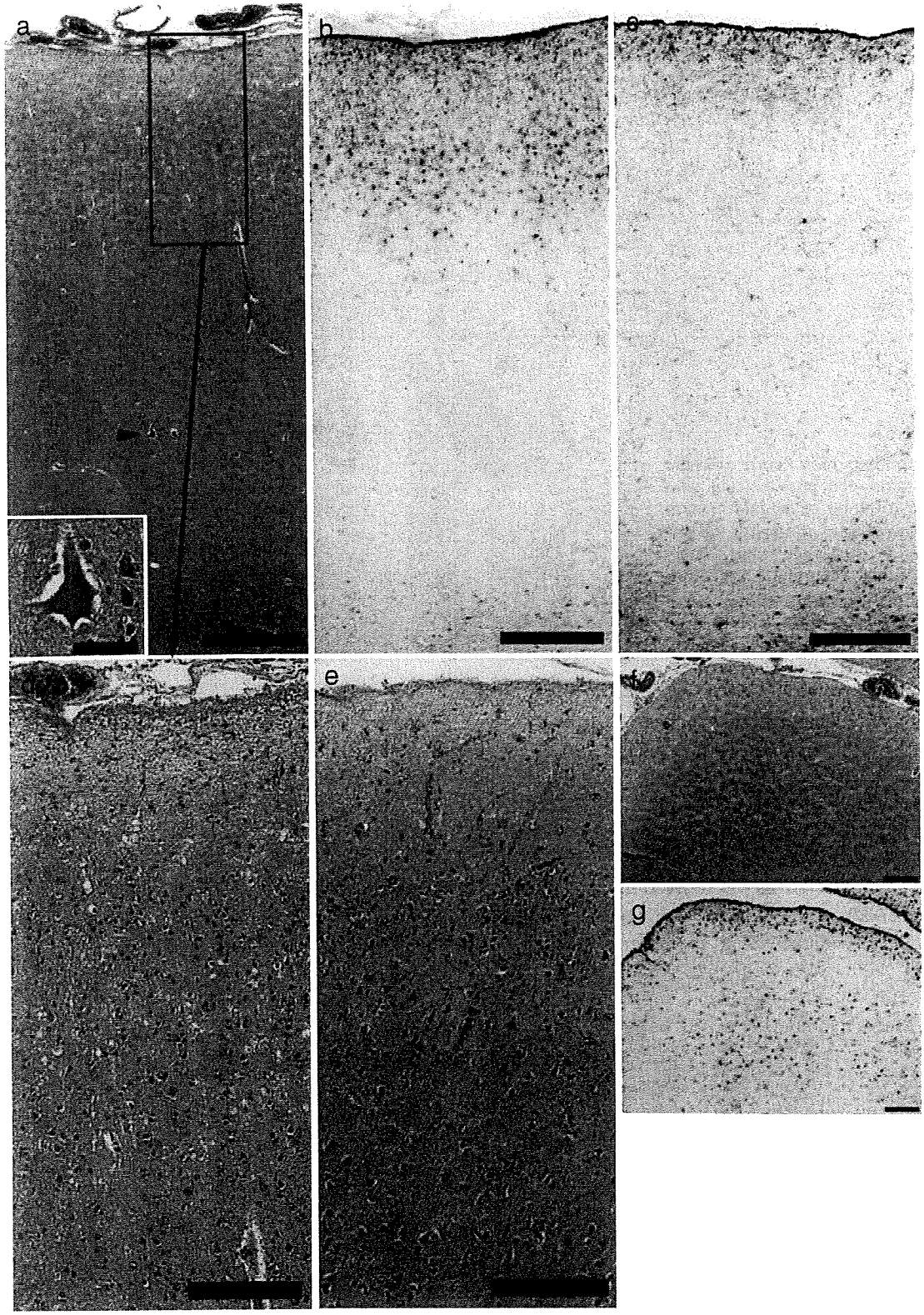

Fig. 4 (a) and (b) are serial sections. (a,b) Laminar cortical necrosis with vacuoles (a) and astrocytosis (b) in the second and third layers of the left primary motor cortex, with some vacuoles in the first layer (a). Bar = 500 μm. The arrowhead in (a) indicates a Betz cell located in the fifth layer. *Inset* shows this Betz cell. Bar = 50 μm. The area surrounded by the rectangle in (a) is shown in (d). (c) Normally, astrocytes are present only in the first layer of the cerebral cortex (the left postcentral gyrus of the patient). Bar = 500 μm. (d) Neuronal loss in the second and third layers. Bar = 200 μm. (e) There are no abnormalities in the second and third layers of the left postcentral gyrus. Bar = 200 μm. (f), (g) Another cortical lesion. Bar = 200 μm. (a), (d–f) HE stain, (b, c, g) GFAP stain.

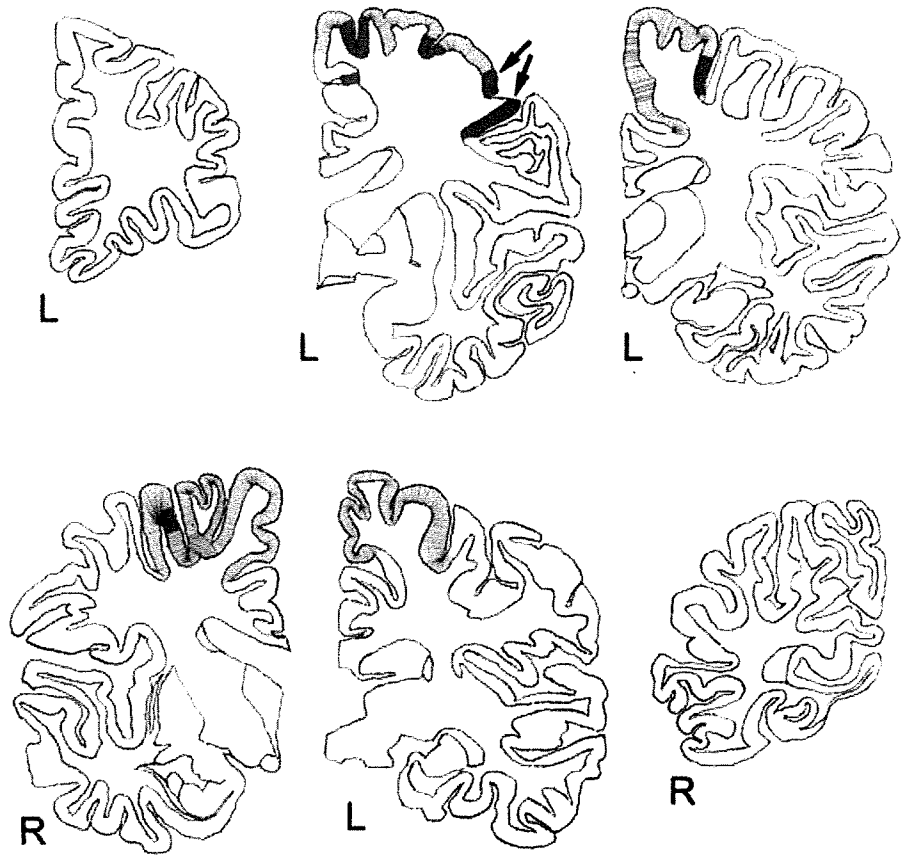

Fig. 5 The primary motor cortices where Betz cells were seen are depicted with lines. The distribution of laminar cortical necrosis with vacuoles and astrocytosis is shown in red. The lesions were mainly located in the bilateral primary motor cortices. On the left side, the lower part of the primary motor cortex was involved (arrows).

encephalopathy is characterized by central chromatolysis of the neurons in the pontine nucleus, where they are constant, in the cerebellar dentate nuclei, nuclei of cranial nerves, gracile and cuneate nuclei, and Betz cells.[14] The central chromatolysis in pellagra is thought to be not a retrograde change but a primary cytoplasmic change.[14]

Morel's laminar sclerosis was derived from the publication by Morel describing unusual pathological changes in four alcoholics, demonstrating spongiform change and astrocytosis seen extensively and symmetrically in the cerebral cortex, mostly confined to the third layer.[2] The review of Morel's laminar sclerosis published by Okeda *et al.* in 1976[5] described 21 cases of Morel's laminar sclerosis, in which Marchiafava-Bignami disease was seen in 17 cases (81%), and Wernicke's encephalopathy was seen in six cases (30%). They reported that Morel's laminar sclerosis was not seen in the occipital lobe. In their own case, laminar astrocytosis was seen in the third layer of the frontal, parietal, and temporal cortex. Spongiform changes were observed in the adjacent second layer. The lesions were severe in the middle and inferior frontal gyri.[5] Since 1976, three papers have reported patients with Morel's laminar sclerosis in the English language literature.[3,4,6] Naeije *et al.* reported that the lesions selectively involved the third and fourth layers of the cortex. Characteristic changes were neuronal loss, capillary proliferation with thickened endothelia, proliferation of microglial cells, and swollen astrocytes.[3] Okeda *et al.* reported that the cerebral cortex presented extensive laminar astrocytosis and/or laminar neuronal loss accompanied by capillary proliferation in the middle layers of the frontal and parietal cortices in case 2.[4] Sato *et al.* reported that the cerebral cortices showed mild neuronal loss and proliferation of astrocytes, particularly in the third layer.[6]

Recently, by application of MRI, cortical involvement in patients with Wernicke's encephalopathy or Marchiafava-Bignami disease has been increasingly reported.[11,15-22] Interestingly, the primary motor cortex was involved in most of these cases while the description regarding focal neurological signs was absent. In other words, the regions around the primary motor cortex seem to be sometimes mildly involved in these diseases. Although these reports did not include detailed histological findings, the cortical lesions may reflect Morel's laminar sclerosis[17] or hepatocerebral degeneration.[23]

To date, clinicopathological correlation in Morel's laminar sclerosis has rarely been reported, probably because consciousness disturbance due to concomitant Wernicke's encephalopathy or Marchiafava-Bignami disease masks the symptoms. In our case, spontaneous

speech was impossible on admission, but comprehension of spoken language was good. After the disappearance of consciousness disturbance, we found that the written language was normal, even though the disturbance in speech output was not completely resolved. Although neuropsychological tests were not performed in detail, we considered that his speech disturbance was AOS. The concept of AOS has been controversial and is sometimes called pure anarthrica[24] or aphemia.[7,25] AOS is caused by disturbance of motor programming of articulation, and is classically distinguished from Broca's aphasia by the preservation of ability to write language.[7] The differentiation of AOS from dysarthria is also sometimes difficult. In our case, tongue protrusion was impossible, but speech disturbance was significantly worse than expected. Although AOS has been reported to be caused by brain lesions involving various areas,[7,24-27] one of the responsible areas is the lower part of the left primary motor cortex.[25-27]

In conclusion, we report a patient with Morel's laminar sclerosis in whom AOS was seen. Involvement of the lower part of the left primary motor cortex may be associated with AOS in our case.

ACKNOWLEDGMENT

The authors thank Dr Satoru Ishibashi (Department of Neurology and Neurological Science, Graduate School, Tokyo Medical and Dental University) for help for the production of the manuscript, and Ms Hiromi Kondo (Tokyo Institute of Psychiatry) for excellent technical assistance. This work was supported by a grant-in-aid for scientific research from the Ministry of Education, Culture, Sports, Science and Technology (14570957) and a research grant from the Zikei Institute of Psychiatry.

REFERENCES

1. Tsuchiya K, Takahashi M, Ikeda K. Subacute speech apraxia and consciousness disturbance in a 57-year-old non-alcoholic man. *Neuropathology* 2003; **23**: 360–363.
2. Morel F. Une Forme anatomo-clinique particulière de l'alcoolisme chronique: Sclérose corticale laminaire alcoolique. *Rev Neurol (Paris)* 1939; **71**: 280–288.
3. Naeije R, Franken L, Jacobovitz D, Flament-Durand J. Morel's laminar sclerosis. *Eur Neurol* 1978; **17**: 155–159.
4. Okeda R, Kitano M, Sawabe M, Yamada I, Yamada M. Distribution of demyelinating lesions in pontine and extrapontine myelinolysis – three autopsy cases including one case devoid of central pontine myelinolysis. *Acta Neuropathol* 1986; **69**: 259–266.
5. Okeda R, Nakano T. An autopsy case of chronic alcoholism with alcoholic laminar cortical sclerosis (Morel) and so-called pellagra encephalopathy – some clinical and pathological comments about each changes. *Shinkei Kenkyu No Shimpo* 1976; **20**: 385–399 (in Japanese).
6. Sato Y, Tabira T, Tateishi J. Marchiafava-Bignami disease, striatal degeneration, and other neurological complications of chronic alcoholism in a Japanese. *Acta Neuropathol* 1981; **53**: 15–20.
7. Fox RJ, Kasner SE, Chatterjee A, Chalela JA. Aphemia: an isolated disorder of articulation. *Clin Neurol Neurosurg* 2001; **103**: 123–126.
8. Sechi G, Serra A. Wernicke's encephalopathy: new clinical settings and recent advances in diagnosis and management. *Lancet Neurol* 2007; **6**: 442–455.
9. Torvik A. Two types of brain lesions in Wernicke's encephalopathy. *Neuropathol Appl Neurobiol* 1985; **11**: 179–190.
10. Okeda R, Taki K, Ikari R, Funata N. Vascular changes in acute Wernicke's encephalopathy. *Acta Neuropathol* 1995; **89**: 420–424.
11. Zhong C, Jin L, Fei G. MR imaging of nonalcoholic Wernicke encephalopathy: a follow-up study. *AJNR Am J Neuroradiol* 2005; **26**: 2301–2305.
12. Park SH, Na DL, Lee JH *et al.* Alcoholic pellagra encephalopathy combined with Wernicke disease. *J Korean Med Sci* 1991; **6**: 87–93.
13. Serdaru M, Hausser-Hauw C, Laplane D *et al.* The clinical spectrum of alcoholic pellagra encephalopathy. A retrospective analysis of 22 cases studied pathologically. *Brain* 1988; **111**: 829–842.
14. Hauw JJ, De Baecque C, Hausser-Hauw C, Serdaru M. Chromatolysis in alcoholic encephalopathies. Pellagra-like changes in 22 cases. *Brain* 1988; **111**: 843–857.
15. Fei GQ, Zhong C, Jin L *et al.* Clinical characteristics and MR imaging features of nonalcoholic Wernicke encephalopathy. *AJNR Am J Neuroradiol* 2008; **29**: 164–169.
16. Ihn YK, Hwang SS, Park YH. Acute Marchiafava-Bignami disease: diffusion-weighted MRI in cortical and callosal involvement. *Yonsei Med J* 2007; **48**: 321–324.
17. Johkura K, Naito M, Naka T. Cortical involvement in Marchiafava-Bignami disease. *AJNR Am J Neuroradiol* 2005; **26**: 670–673.
18. Kim MJ, Kim JK, Yoo BG, Kim KS, Jo YD. Acute Marchiafava-Bignami disease with widespread callosal and cortical lesions. *J Korean Med Sci* 2007; **22**: 908–911.
19. Kinoshita Y, Inoue Y, Tsuru E, Yasukouchi H, Yokota A. Unusual MR findings of Wernicke encephalopathy with cortical involvement. *No To Shinkei* 2001; **53**: 65–68 (in Japanese with English abstract).

20. Ménégon P, Sibon I, Pachai C, Orgogozo JM, Dousset V. Marchiafava-Bignami disease: diffusion-weighted MRI in corpus callosum and cortical lesions. *Neurology* 2005; **65**: 475–477.
21. Tuntiyatorn L, Laothamatas J. Acute Marchiafava-Bignami disease with callosal, cortical, and white matter involvement. *Emerg Radiol* 2008; **15**: 137–140.
22. Yamashita M, Yamamoto T. Wernicke encephalopathy with symmetric pericentral involvement: MR findings. *J Comput Assist Tomogr* 1995; **19**: 306–308.
23. Jog MS, Lang AE. Chronic acquired hepatocerebral degeneration: case reports and new insights. *Mov Disord* 1995; **10**: 714–722.
24. Tabuchi M, Odashima K, Fujii T, Suzuki K, Saitou J, Yamadori A. The left central gyral lesion and pure anarthria (In Japanese with English abstract). *Rinsho shinkeigaku* 2000; **40**: 464–470.
25. Schiff HB, Alexander MP, Naeser MA, Galaburda AM. Aphemia Clinical-anatomic correlations. *Arch Neurol* 1983; **40**: 720–727.
26. Josephs KA, Duffy JR, Strand EA *et al.* Clinicopathological and imaging correlates of progressive aphasia and apraxia of speech. *Brain* 2006; **129**: 1385–1398.
27. Otsuki M. Aphasia in practice – recent progress. *Rinsho Shinkeigaku* 2008; **48**: 853–856 (in Japanese with English abstract).

Journal of the Neurological Sciences 285 (2009) 241–245

Contents lists available at ScienceDirect

Journal of the Neurological Sciences

journal homepage: www.elsevier.com/locate/jns

Short c ication

Intractable hiccup caused by medulla oblongata lesions: A study of an autopsy patient with possible neuromyelitis optica

Zen Kobayashi [a,b,*], Kuniaki Tsuchiya [b,c], Toshiki Uchihara [d], Ayako Nakamura [d], Chie Haga [b], Osamu Yokota [b,e], Hideki Ishizu [f], Kazuhiro Taki [g], Tetsuaki Arai [b], Haruhiko Akiyama [b], Hidehiro Mizusawa [a]

[a] Department of Neurology and Neurological Science, Graduate School, Tokyo Medical and Dental University, Tokyo, 113-8519, Japan
[b] Tokyo Institute of Psychiatry, Tokyo, 156-8585, Japan
[c] Department of Laboratory Medicine and Pathology, Tokyo Metropolitan Matsuzawa Hospital, Tokyo, 156-0057, Japan
[d] Department of Neurology, Tokyo Metropolitan Institute for Neuroscience, Tokyo, 183-8526, Japan
[e] Department of Neuropsychiatry, Okayama University Graduate School of Medicine, Dentistry and Pharmaceutical Sciences, Okayama, 700-8558, Japan
[f] Department of Laboratory Medicine, Zikei Institute of Psychiatry, Okayama, 702-8508, Japan
[g] Department of Pathology, Musashino Redcross Hospital, Tokyo 180-8610, Japan

ARTICLE INFO

Article history:
Received 23 March 2009
Received in revised form 17 May 2009
Accepted 9 June 2009
Available online 3 July 2009

Keywords:
Intractable hiccup
Nucleus tractus solitarius
Multiple sclerosis
Neuromyelitis optica

ABSTRACT

We report the first autopsy verification of medulla oblongata lesions involving bilateral nucleus tractus solitarius (NTS) as a cause of intractable hiccup in an autopsy patient. The female patient first developed pain and weakness in the lower limbs and urinary incontinence at age 48, and was given a diagnosis of myelitis. Intractable hiccup was accompanied by urinary retention on the third attack. She died of respiratory failure when the fifth attack occurred at age 51. Autopsy disclosed severe involvement of the medulla oblongata and entire spinal cord. Optic nerve lesions were also identified unexpectedly. Dual involvement of the optic nerve and spinal cord, necrotic spinal cord lesions involving not only myelin but also neurons and axon, and marked extension of the spinal cord lesions in both the longitudinal and transverse directions suggested the diagnosis of neuromyelitis optica rather than multiple sclerosis. Although animal experiments have shown that NTS is a critical structure in the hiccup reflex, we demonstrated for the first time the involvement of the NTS in an autopsy patient with intractable hiccup.

1. Introduction

Hiccup is a repetitive involuntary, spasmodic, and temporary contraction of the diaphragm accompanied by sudden closure of the glottis [1], which is mediated through the center located in the medulla oblongata [2]. In neuromyelitis optica (NMO), involvement of medulla oblongata has been reported [3–7], and clinical observations suggest a possible link with intractable hiccup. Recently, Misu et al. reported that intractable hiccup was found in eight of 47 cases of relapsing NMO but in none of 130 cases of multiple sclerosis (MS) [4].

There has been a long controversy as to whether NMO is a variant of MS or a distinct disease [8]. However, recent serological findings strongly suggest that NMO is a distinct disease that has characteristic clinical and pathological features [9]. The main target antigen is aquaporin 4 (AQP4) that is a water channel protein located in the astrocytic foot process. AQP4 is found on all surfaces of astrocytes, but occurs at the highest concentration in the perivascular and peripial end-feet, and ependymal-cell membranes. In the nervous system, AQP4 is predominantly expressed within optic nerves, spinal cord, and periventricular regions such as brainstem and hypothalamus, and this correlates with the predominant lesion sites in NMO [10]. Histopathologically, AQP4 immunoreactivity is undetectable at the lesions of NMO [6,8,11] in contrast to MS [8,11,12]. Here, we demonstrated the involvement of the nucleus tractus solitarius (NTS) in a patient with possible NMO who developed intractable hiccup.

2. Case report

A 48-year-old woman noticed pain around the left triceps muscle of the calf, weakness at the distal portion of the right leg and urinary incontinence within 3 weeks prior to admission to our hospital. Neurological examination disclosed distal weakness and hyperreflexia in the bilateral lower limbs with hypesthesia below the S2 dermatome. Hyperintensities at the cervical cord were noted on T2-weighted image. Cerebrospinal fluid (CSF) examination showed pleocytosis (cell count 237/mm^3, mononuclear cells 190, polymorphonuclear cells 47), total protein 44 mg/dl, IgG 12 mg/dl (normal range: 0.5–4) and oligoclonal IgG band. Subsequently, weakness in the right upper limb, hyperreflexia in the bilateral upper and lower limbs, sensory disturbance below the C5 dermatome, urinary retention, and constipation appeared. She was given

* Corresponding author. Tokyo Institute of Psychiatry, 2-1-8 Kamikitazawa, Setagayaku, Tokyo, Japan, 156-8585. Tel.: +81 3 3304 5701; fax: +81 3 3329 8035.
E-mail address: zen@bg7.so-net.ne.jp (Z. Kobayashi).

0022-510X/$ – see front matter © 2009 Elsevier B.V. All rights reserved.
doi:10.1016/j.jns.2009.06.014

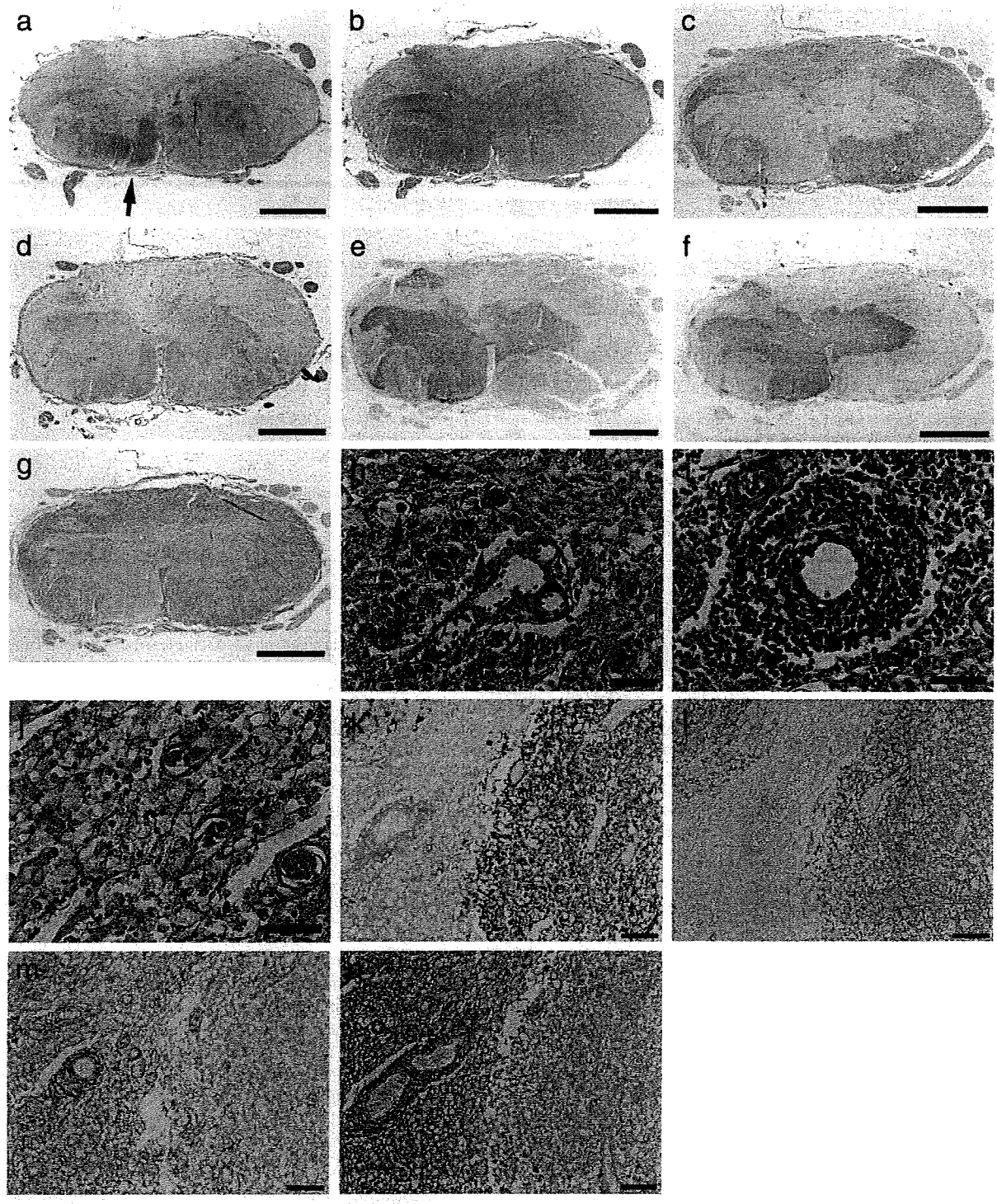

Fig. 1. Cervical cord (C7). Extensive myelin pallor was seen, and boundaries between the gray and white matter were unclear (a). Only the right anterior column (a, arrow) was relatively preserved. Extensive axonal loss was seen in the white matter (b). Macrophages dispersed mainly in the white matter (c). In the lesions where macrophages dispersed, immunoreactivity for MBP (d) was decreased, and that for GFAP (e) and AQP4 (f) was undetectable. Immunoreactivity for IgM was conversely strong in this lesion (g). Capillary proliferation and spheroids (h, arrow) were seen in the lesion (h). Perivascular lymphocytic proliferation was seen in the lesion (i). Infiltrating cells of the parenchyma were mainly lipid-laden macrophages (j). (k)–(n) are serial sections. The left half of the each figure corresponds to the lesion. In the lesion, immunoreactivity for GFAP (k) and AQP4 (l) was undetectable except for the left upper corner. Conversely, immunoreactivity for IgM (m) and IgG (n) was strong in the lesion, and prominent in the perivascular area. Scale bar: a–g 3 mm, h–j 50 μm, k–n 100 μm. a KB stain, b Bodian stain, c–g, k–n immunohistochemistry (c CD68, d MBP, e, k GFAP, f, l AQP4, g, m IgM, n IgG), h–j H&E stain.

a diagnosis of myelitis, and was treated with methylprednisolone pulse therapy. The treatment was effective and followed by oral prednisolone of 60 mg/day, which was tapered off by day 82. On day 113, exacerbation of gait disturbance occurred, and neurological examination demonstrated impaired position sense of the lower limbs. The entire clinical course suggested MS. After clinical improvement with prednisolone 30 mg/day, she could walk with a stick. On day 619, she noticed exacerbation of urinary retention, and on day 624, hiccup emerged. CSF and brain MRI appeared normal. Urinary retention and hiccups improved without any treatment within two weeks. On day 662, dysarthria and dysphagia appeared, and this exacerbation was complicated with respiratory failure due to bronchopneumonia. She required mechanical

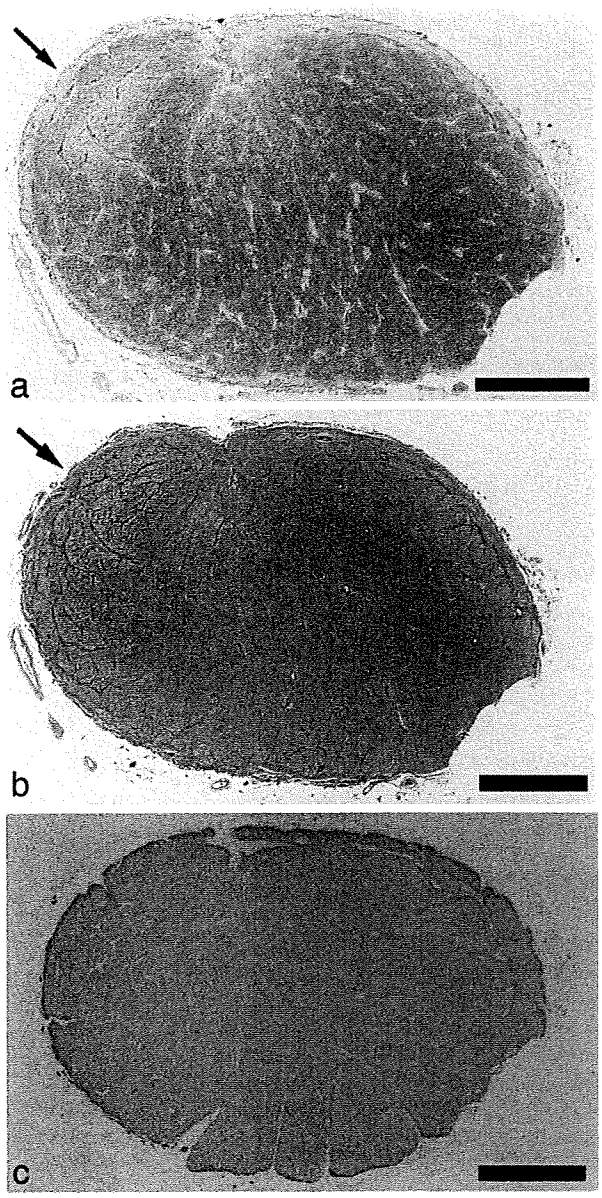

Fig. 2. Coronal section of the right optic nerve. Myelin pallor (a, arrow) and collagen proliferation (b, arrow) were demonstrated, but cellular infiltration was not seen. AQP4 loss was not apparent in this lesion (c). Scale bar: a–c 1 mm. a KB stain, b H&E stain, c AQP4.

ventilatory assistance through a tracheotomy tube, but was successfully weaned on day 692. Thereafter, however, she remained bedridden, and needed intravenous hyperalimentation because of the dysphagia. Although her symptoms stabilized, paralysis of the right upper limb appeared on day 1050, and weakness of lower limbs progressed. Cell count of the CSF was 29/mm^3, total protein 144 mg/dl, and IgG 25.8 mg/dl. The clinical course was complicated by bronchopneumonia, which became fatal on day 1065. Throughout her clinical course, there was no visual manifestation. General autopsy findings were unremarkable except for bronchopneumonia of the left lower lobe.

3. Neuropathological findings

Brain weight was 1280 g after fixation. Samples were fixed with 10% formalin and embedded in paraffin. Ten-μm-thick sections were prepared from the bilateral optic nerves, cerebrum, midbrain, pons, medulla oblongata, cerebellum, and spinal cord (C6, C7, C8, Th3, Th6, Th10, L3, L5, and S1). These sections were stained with hematoxylin–eosin (H&E) and Klüver–Barrera (KB). For immunohistochemistry, we prepared four-μm-thick sections, and used anti-CD68 (KP1, mouse, monoclonal Dako, 1:100), anti-glial fibrillary acidic protein (GFAP) (rabbit, polyclonal, Dako, 1:1000), anti-myelin basic protein (MBP) (rabbit, polyclonal, IBL, 1:100), anti-IgM (rabbit, polyclonal, Cappel, 1:1000), anti-IgG (rabbit, polyclonal, Dako, 1:250), and anti-AQP4 (rabbit, polyclonal, Santa Cruz, 1:500) antibodies. To evaluate of the lesions of the medulla oblongata, sections from a neurologically normal control (67-year-old woman) were also prepared.

External macroscopic examination of the leptomeninges was unremarkable. On sections, the cerebrum, cerebellum, midbrain, and pons were unremarkable. In the medulla oblongata, the dorsal portion adjacent to the fourth ventricle appeared gray. In the cervical cord, the lateral and posterior columns partly appeared gray, and were sclerotic. In the cervical and thoracic cord, boundaries between the gray and white matter were unclear.

On microscopic examination, lesions were seen in all sections of the spinal cord and medulla oblongata. In all sections of the spinal cord, the lesions involved both the gray and white matter in almost the same degree, although the active lesions of the lower cervical cord preferentially involved the white matter (Fig. 1). The lesions occupied more than half the area of the spinal cord. In the bilateral optic nerves, myelin pallor and collagen proliferation was demonstrated (Fig. 2). In the lesions of the spinal cord, myelin, axon, and neurons were reduced. Capillary proliferation and cellular infiltration were seen in the sections at the level of the medulla oblongata (only in the lowest portion), and cervical and sacral cord. Proliferating cells were macrophages and lymphocytes (Fig. 1i, j). In contrast, cellular infiltration was not evident at the thoracic and lumbar cord. In the section of the lumbar cord (L5), there was a motor neuron loss in the right anterior horn, probably related to motor paralysis occurring at disease onset. In the active lesions of the cervical cord (C7) where macrophages dispersed, immunoreactivity for MBP was decreased, and that for GFAP and AQP4 was undetectable (Fig. 1e, f). In contrast, strong immunoreactivity for IgM and IgG was present in this lesion (Fig. 1g, m, n). AQP4 loss was not demonstrated in the inactive lesions of the optic nerve, medulla oblongata, thoracic and lumbar cord where cellular infiltration was not seen (Fig. 2). In the medulla oblongata, the dorsal and pericanal region, right inferior olivary nucleus, and bilateral medial lemniscus were involved (Fig. 3). The dorsal and pericanal lesions affected the bilateral hypoglossal nucleus, dorsal vagal nucleus, and NTS. Neurons of the bilateral hypoglossal nucleus, dorsal vagal nucleus, NTS, and right inferior olivary nucleus were reduced. The neurons of the nucleus ambiguus were not identifiable in either sample from our case or that from the normal control, but the regions where the nucleus ambiguus is thought to be located were not involved in the patient.

4. Discussion

Clinical features of this patient are characterized by recurrent myelitis, later complicated by bulbar dysfunctions, manifesting as intractable hiccup, respiratory failure, and dysphagia. Clinically, our case did not fulfill the diagnostic criteria of NMO [13] because there were no visual manifestations throughout the clinical course. Further, serum antibodies to AQP4 could not be measured. Abnormalities of the optic nerves might have been detected if visual evoked potentials were examined. On the other hand, optic nerve lesions were unexpectedly identified at autopsy. Dual involvement of the optic nerve and spinal cord, necrotic spinal cord lesions involving not only myelin but also neurons and axon, and marked extension of the spinal cord lesions in both the longitudinal and transverse directions suggested the diagnosis of NMO rather than MS.

Clinically, NMO usually begins with either optic neuritis or myelitis, and can manifest as isolated myelitis [10] or optic neuritis [14]. NMO usually follows a relapsing course. Recently, Misu et al. reported that intractable hiccup was found in 17% of patients with relapsing NMO [4]. Respiratory failure caused by ascending cervical myelitis is the most

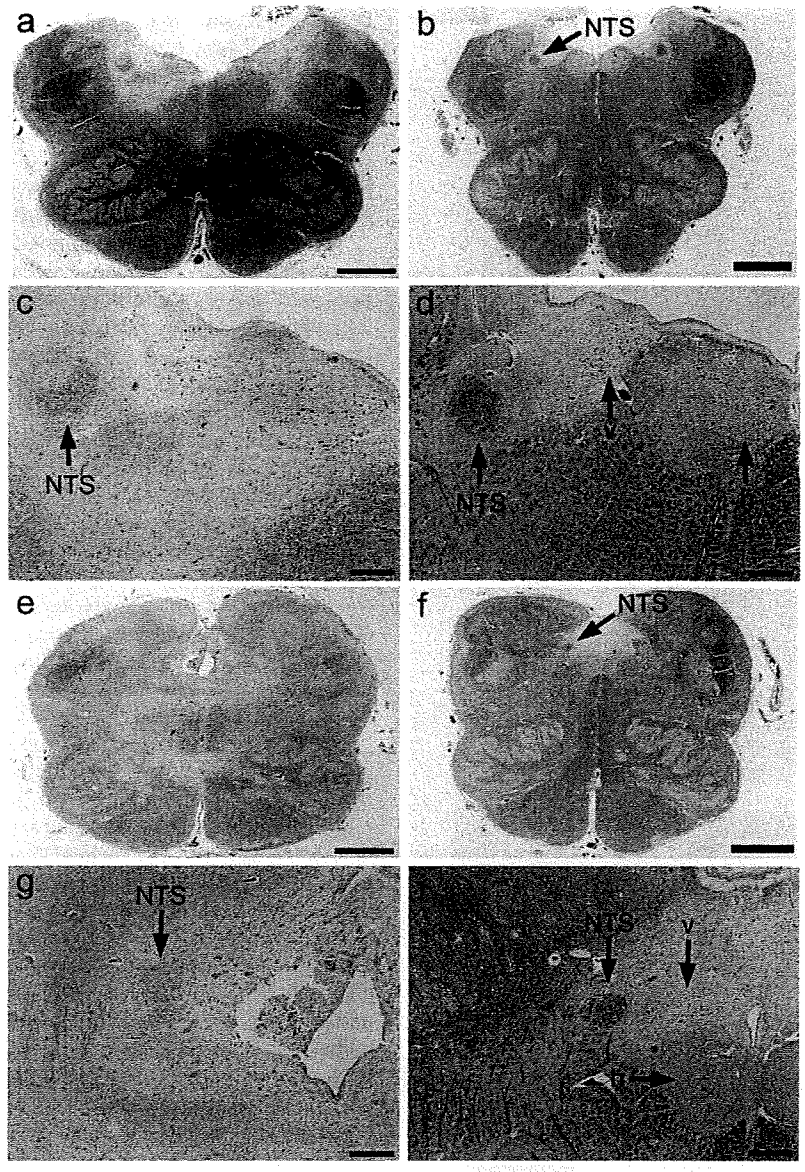
a
b
NTS
c
NTS
d
NTS
V
e
f
NTS
g
NTS
NTS
V

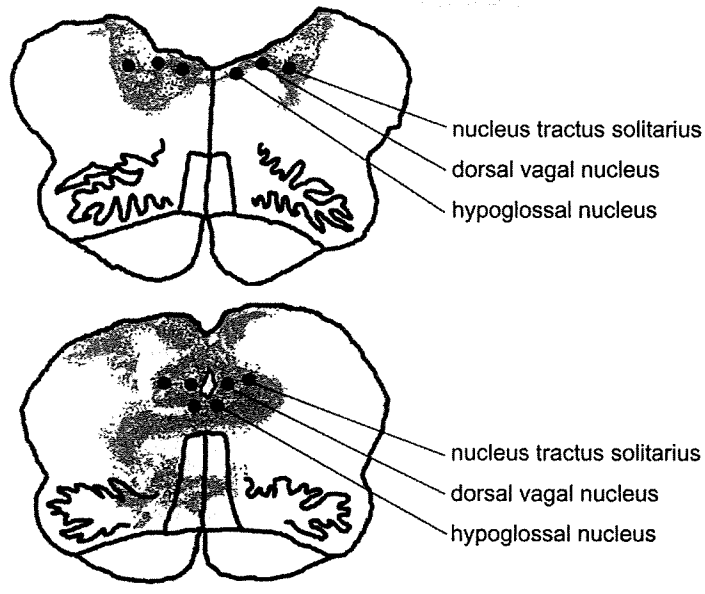
nucleus tractus solitarius
dorsal vagal nucleus
hypoglossal nucleus
nucleus tractus solitarius
dorsal vagal nucleus
hypoglossal nucleus

frequent cause of death [15]. Relapsing NMO has a marked female predominance and a 5-year survival rate of 70% [15]. CSF analysis shows mixed mononuclear and polymorphonuclear pleocytosis. The total cell count exceeds 50/mm^3 during relapses, however, in contrast to MS, the cell count is normal or near normal during remissions. Oligoclonal bands are positive in about 35% of cases [10]. In MRI, the hallmark of NMO is spinal cord lesions extending over three or more vertebral segments. Pittock et al. reported MRI lesions of NMO were sometimes seen around the third and fourth ventricle, and the aqueduct of Sylvius. These lesions involved brainstem and hypothalamus [5]. Li et al. also reported that the brainstem was a frequently involved region (42.4%), especially in the medulla (21.2%) [3]. Histopathologically, AQP4 loss within spinal cord lesions appears to be a consistent finding in NMO [6,8,11], although AQP4 is sometimes present in chronic inactive lesions [8]. Foci of AQP4 loss in NMO corresponds well with the site of immunoglobulin and complement activation as we observed in our patient. If the diffuse infiltration of macrophages in the lower cervical cord in our patient represents a feature of "active demyelinating lesion" of NMO [8], concomitant loss of MBP, GFAP, and AQP4 immunoreactivities further characterizes these lesions as representative of an early stage of NMO [8]. It remains to be clarified, however, whether similar loss of these immunoreactivities, not observed in conventional MS lesions, is also characteristic of NMO even with some necrotic features as seen in the cervical cord lesion in our patient. Because Roemer et al. reported that proliferative astrocytic response was seen regardless of the stage of demyelinating activity [6], relative paucity of AQP4 may possibly represent a pathological feature of NMO.

Dorsal and pericanal regions of the medulla oblongata are frequently involved in NMO. One of the explanations for this regional preference is the relative abundance of AQP4 expression and compromised blood-brain barrier (BBB) functions in these areas [6,8,10]. However, in contrast to the severe clinical manifestations of lesions that involve the spinal cord or optic nerves, medullary lesions usually remain clinically silent [5] or only cause intractable hiccup [4], and showed resolution on MRI in some patients [4,5]. Roemer et al. reported that the dorsal medullary lesion in NMO showed cellular infiltration and IgM deposition without demyelination or necrosis [6].

Hiccup lasting for more than 48 h is defined as "intractable" [1]. To date, mechanisms of hiccup have been studied mainly by animal experiments. The afferent pathway of hiccup is composed of the sensory fibers of the vagal nerve, pharyngeal branch of the grossopharyngeal nerve, pharyngeal plexus from C2 to C4, and sympathetic nerves from Th6 to Th12 [2,16,17]. Although the details are not well known, triggering signals are conveyed through these afferents to the NTS [18], and then to the nucleus ambiguus located in more ventrolateral part. The NTS is located along the length of the medulla, with a small portion in the lower pons. The solitary tract runs in the middle of the nucleus, creating a speck of white matter, surrounded by gray matter (the nucleus). This stands out on a stained section, which is where the name solitary comes from (Fig. 2b, f). The nucleus received fibers from the tractus solitarius, which contains afferent fibers from the glossopharyngeal and vagal nerves. These fibers convey visceral impulses from the pharynx (glossopharyngeal and vagal nerves), and from the esophagus and abdominal alimentary canal (vagal nerve). Ventral and interstitial subnuclei receive tracheal, laryngeal and pulmonary afferents and play an important role in both respiratory control and rhythm generation [18]. The efferent pathway of hiccup consists of the phrenic nerves to the diaphragm, the external intercostal nerves (Th1–Th11) to the intercostal muscles, and the scalenus anticus nerve to the scalene muscle which elevate the clavicles. Thirty-five milliseconds after inspiratory activation, the recurrent nerve (from the vagal nerve) affects glottis closure, resulting in the characteristic "hic" [2]. Regarding central hiccups, a medullary lesion is thought to cause hiccup, and the underlying diseases are ischemic stroke, megadolichobasilar artery, tumors, encephalitis [19], and NMO [4,7]. However, to date, a medullary lesion causing hiccup has been investigated by autopsy neither in NMO nor in other diseases. In our case, the bilateral NTS were involved, without extension into more ventrolateral areas containing the nucleus ambiguus. Lack of cellular infiltration in this lesion suggests its chronic nature, which is in agreement with the appearance of hiccup one year prior to death.

In conclusion, we demonstrated for the first time the involvement of the NTS in a patient with intractable hiccup. This report on a possible NMO patient provides the first autopsy verification of NTS lesion relevant to intractable hiccup.

Acknowledgements

The authors thank Yo Shoda and Kyoko Suzuki for the excellent photographic assistance.

This work was supported by a grant-in-aid for scientific research from the Ministry of Education, Culture, Sports, Science and Technology (14570957) and a research grant from the Zikei Institute of Psychiatry.

References

[1] McFarling DA, Susac JO. Hoquet diabolique: intractable hiccups as a manifestation of multiple sclerosis. Neurology 1979;29:797–801.
[2] Kahrilas PJ, Shi G. Why do we hiccup? Gut 1997;41:712–3.
[3] Li Y, Xie P, Lv F, Mu J, Li Q, Yang Q, et al. Brain magnetic resonance imaging abnormalities in neuromyelitis optica. Acta Neurol Scand 2008;118:218–25.
[4] Misu T, Fujihara K, Nakashima I, Sato S, Itoyama Y. Intractable hiccup and nausea with periaqueductal lesions in neuromyelitis optica. Neurology 2005;65:1479–82.
[5] Pittock SJ, Weinshenker BG, Lucchinetti CF, Wingerchuk DM, Corboy JR, Lennon VA. Neuromyelitis optica brain lesions localized at sites of high aquaporin 4 expression. Arch Neurol 2006;63:964–8.
[6] Roemer SF, Parisi JE, Lennon VA, Benarroch EE, Lassmann H, Bruck W, et al. Pattern-specific loss of aquaporin-4 immunoreactivity distinguishes neuromyelitis optica from multiple sclerosis. Brain 2007;130:1194–205.
[7] Takahashi T, Miyazawa I, Misu T, Takano R, Nakashima I, Fujihara K, et al. Intractable hiccup and nausea in neuromyelitis optica with anti-aquaporin-4 antibody: a herald of acute exacerbations. J Neurol Neurosurg Psychiatry 2008;79:1075–8.
[8] Misu T, Fujihara K, Kakita A, Konno H, Nakamura M, Watanabe S, et al. Loss of aquaporin 4 in lesions of neuromyelitis optica: distinction from multiple sclerosis. Brain 2007;130:1224–34.
[9] Lennon VA, Wingerchuk DM, Kryzer TJ, Pittock SJ, Lucchinetti CF, Fujihara K, et al. A serum autoantibody marker of neuromyelitis optica: distinction from multiple sclerosis. Lancet 2004;364:2106–12.
[10] Jarius S, Paul F, Franciotta D, Waters P, Zipp F, Hohlfeld R, et al. Aquaporin-4 antibodies in neuromyelitis optica. Nat Clin Pract Neurol 2008;4:202–14.
[11] Sinclair C, Kirk J, Herron B, Fitzgerald U, McQuaid S. Absence of aquaporin-4 expression in lesions of neuromyelitis optica but increased expression in multiple sclerosis lesions and normal-appearing white matter. Acta Neuropathol 2007;113:187–94.
[12] Aoki-Yoshino K, Uchihara T, Duyckaerts C, Nakamura A, Hauw JJ, Wakayama Y. Enhanced expression of aquaporin 4 in human brain with inflammatory diseases. Acta Neuropathol 2005;110:281–8.
[13] Wingerchuk DM, Lennon VA, Pittock SJ, Lucchinetti CF, Weinshenker BG. Revised diagnostic criteria for neuromyelitis optica. Neurology 2006;66:1485–9.
[14] Matiello M, Lennon VA, Jacob A, Pittock SJ, Lucchinetti CF, Wingerchuk DM, et al. NMO-IgG predicts the outcome of recurrent optic neuritis. Neurology 2008;70:2197–200.
[15] Wingerchuk DM, Hogancamp WF, O'Brien PC, Weinshenker BG. The clinical course of neuromyelitis optica (Devic's syndrome). Neurology 1999;53:1107–14.
[16] Kondo T, Toyooka H, Arita H. Hiccup reflex is mediated by pharyngeal branch of glossopharyngeal nerve in cats. Neurosci Res 2003;47:317–21.
[17] Yamazaki Y, Sugiura T, Kurokawa K. Sinister hiccups. Lancet 2008;371:1550.
[18] Standring S. Gray's anatomy: The anatomical basis of clinical practice. Thirty-Nineth edition. United Kingdom: Churchill Livingstone; 2004. p. 337.
[19] Park MH, Kim BJ, Koh SB, Park MK, Park KW, Lee DH. Lesional location of lateral medullary infarction presenting hiccups (singultus). J Neurol Neurosurg Psychiatry 2005;76:95–8.

Fig. 3. Medulla oblongata of the patient (a, c, e, g) and the normal control (b, d, f, i) stained with KB. (a)–(d) are at the level of caudal end of the fourth ventricle (upper portion of the medulla oblongata). (e)–(g) and (i) are at the level of rostral end of the central canal (lower portion of the medulla oblongata). Normal NTS stands out on the section (b, f). *h* and *v* indicate hypoglossal nucleus and dorsal vagal nucleus, respectively (d, i). Myelin pallor was seen in the dorsal region (a). A high power view demonstrated that the dorsal lesions affected the hypoglossal nucleus, dorsal vagal nucleus, and NTS (c). Myelin pallor was seen in the pericanal region, right inferior olivary nucleus, and bilateral medial lemniscus (e). A high power view demonstrated that the pericanal lesions affected the hypoglossal nucleus, dorsal vagal nucleus, and NTS (g). Scale bar: a, b, e, f 3 mm, c, d, g, i 500 μm. In the lower portion of the figure, schema of medulla oblongata lesions (red) on KB stained sections is shown. Bilateral NTS were involved.

Journal of the Neurological Sciences 277 (2009) 109–113

Contents lists available at ScienceDirect

Journal of the Neurological Sciences

journal homepage: www.elsevier.com/locate/jns

Metastatic CNS lymphoma presenting with periventricular dissemination — MRI and neuropathological findings in an autopsy case

Zen Kobayashi [a,b,*], Kuniaki Tsuchiya [b,c], Akira Machida [d], Jun Goto [e,f], Osamu Yokota [b,g], Hirotomo Miake [h], Sadakiyo Watabiki [i], Kazuhiro Taki [j], Hideki Ishizu [k], Chie Haga [b], Tetsuaki Arai [b], Haruhiko Akiyama [b], Hidehiro Mizusawa [a]

[a] Department of Neurology and Neurological Science, Graduate School, Tokyo Medical and Dental University, Tokyo, 113-8519, Japan
[b] Tokyo Institute of Psychiatry, Tokyo, 156-8585, Japan
[c] Department of Laboratory Medicine and Pathology, Tokyo Metropolitan Matsuzawa Hospital, Tokyo, 156-0057, Japan
[d] Department of Neurology, Nakano General Hospital, Tokyo, 164-0011, Japan
[e] Department of Medicine, Tokyo Metropolitan Matsuzawa Hospital, Tokyo, 156-0057, Japan
[f] Department of Anatomy, Showa University School of Medicine, Tokyo 142-8555, Japan
[g] Department of Neuropsychiatry, Okayama University Graduate School of Medicine, Dentistry and Pharmaceutical Sciences, Okayama, 700-8558, Japan
[h] Department of Neurology, Musashino Redcross Hospital, Tokyo 180-8610, Japan
[i] Musashino Health Development Foundation, Tokyo 180-0001, Japan
[j] Department of Pathology, Musashino Redcross Hospital, Tokyo 180-8610, Japan
[k] Department of Laboratory Medicine, Zikei Institute of Psychiatry, Okayama, 702-8508, Japan

ARTICLE INFO

Article history:
Received 3 September 2008
Received in revised form 15 October 2008
Accepted 29 October 2008
Available online 29 November 2008

Keywords:
Metastatic CNS lymphoma
Periventricular dissemination
MRI
Choroid plexus

ABSTRACT

Metastatic CNS lymphoma usually manifests as pachymeningeal or leptomeningeal infiltrates, and periventricular dissemination is rare. A 70-year old man first noticed a mass in the left supraclavicular fossa, and then presented with bilateral parkinsonism, followed by consciousness disturbance. Fluid attenuated inversion recovery (FLAIR) image of brain MRI demonstrated hyperintensities at the parenchyma around the lateral ventricle, third ventricle, and fourth ventricle. Gadolinium-enhanced T1-weighted image demonstrated enhancement along the whole wall of the ventricle. Biopsy of the left supraclavicular lymph nodes established a diagnosis of diffuse large B-cell lymphoma. The patient died of multiple organ failure about 5 months after the onset. Autopsy disclosed periventricular dissemination of lymphoma cells that was most severe around the lateral ventricle. We considered that the lymphoma cells entered the ventricular system through the choroid plexus of the lateral ventricle, followed by dissemination of the periventricular parenchyma.

1. Introduction

In 5–9% of systemic non-Hodgkin's lymphoma, secondary involvement is seen in the CNS, and usually manifests as pachymeningeal or leptomeningeal infiltrates [1,2]. Parenchymal lesions, when present, typically result from secondary involvement from the leptomeninges [1]. Here, we report an autopsy case of metastatic CNS lymphoma showing an unusual distribution.

2. Case report

A 70-year-old man had noticed a mass in the left supraclavicular fossa, but did not consult a hospital. About 1 month later, he presented with bilateral parkinsonism including gait disturbance, akinesia, mask-like face, and dysphagia. He was admitted to our hospital about 3 months after the onset. Physical examination on admission demonstrated consciousness disturbance with Glasgow Coma Scale (GCS) of 12 (E3 V4 M5), swelling of the left supraclavicular lymph nodes, measured approximately 4 by 5 cm, and was not mobile. Coarse crackles were heard in the lower part of the bilateral lungs. Neurological examination disclosed generalized muscle rigidity including neck rigidity. Blood tests showed lactate dehydrogenase (LDH) of 665 IU/l (normal range: 100–250), soluble interleukin 2 receptor (sIL-2R) 4700 U/ml (normal range <530). Enhanced chest and abdominal CT disclosed swelling of the left supraclavicular, paraaortic, and peritoneal lymph nodes. Galium citrate scintigraphy showed abnormal accumulations in the left supraclavicular area, abdominal cavity, and pelvic cavity. Fluid attenuated inversion recovery (FLAIR) image of brain MRI demonstrated hyperintensities in the parenchyma around the lateral ventricle, third ventricle, and fourth ventricle (Fig. 1). Gadolinium-enhanced T1-weighted image demonstrated abnormal enhancement around the lateral ventricle, third ventricle, fourth ventricle, and pituitary gland, accompanied by low intensity areas at the periventricular parenchyma

* Corresponding author. Tokyo Institute of Psychiatry, 2-1-8 Kamikitazawa, Setagaya-ku, Tokyo, Japan, 156-8585. Tel.: +81 3 3304 5701; fax: +81 3 3329 8035.
E-mail address: zen@bg7.so-net.ne.jp (Z. Kobayashi).

0022-510X/$ – see front matter © 2008 Elsevier B.V. All rights reserved.
doi:10.1016/j.jns.2008.10.029

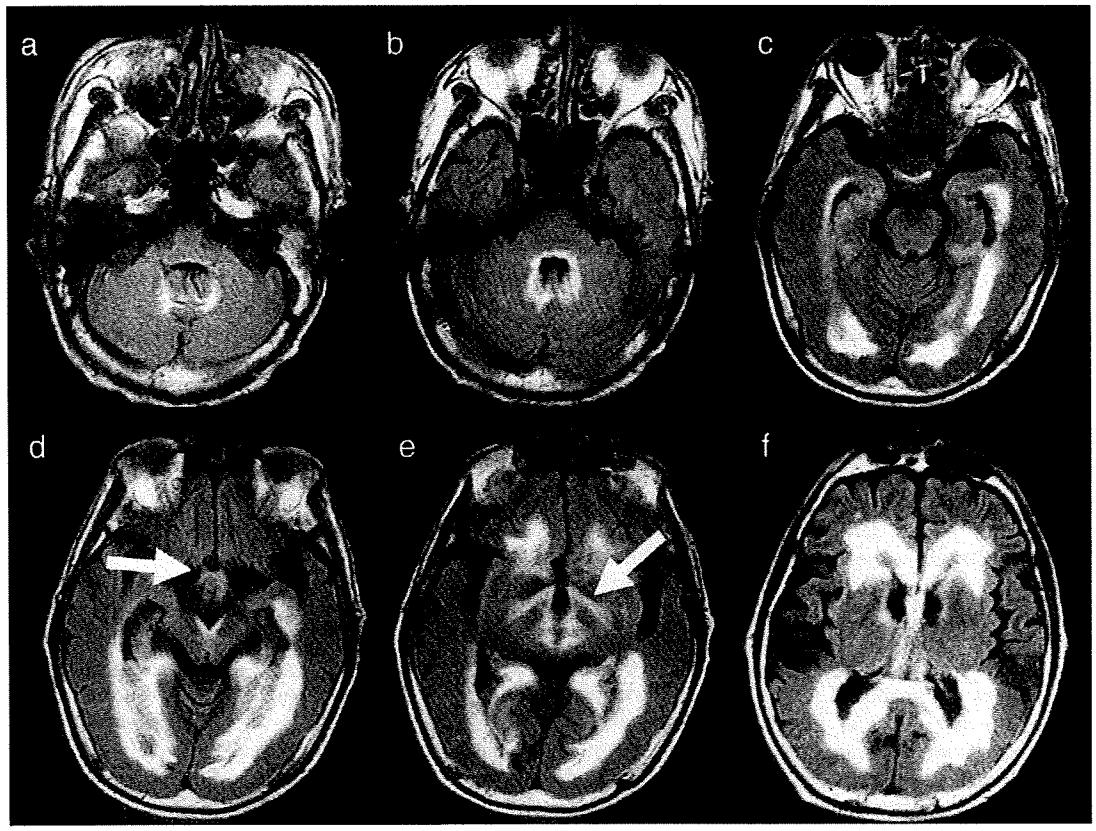

Fig. 1. Fluid attenuated inversion recovery (FLAIR) image demonstrated hyperintensities throughout the periventricular parenchyma. The cerebellum (a), pons (b), cerebral white matter (c–f), midbrain (d), optic chiasma (d, arrow), optic tract (e, arrow), hypothalamus (e), and caudate nucleus (f) were involved.

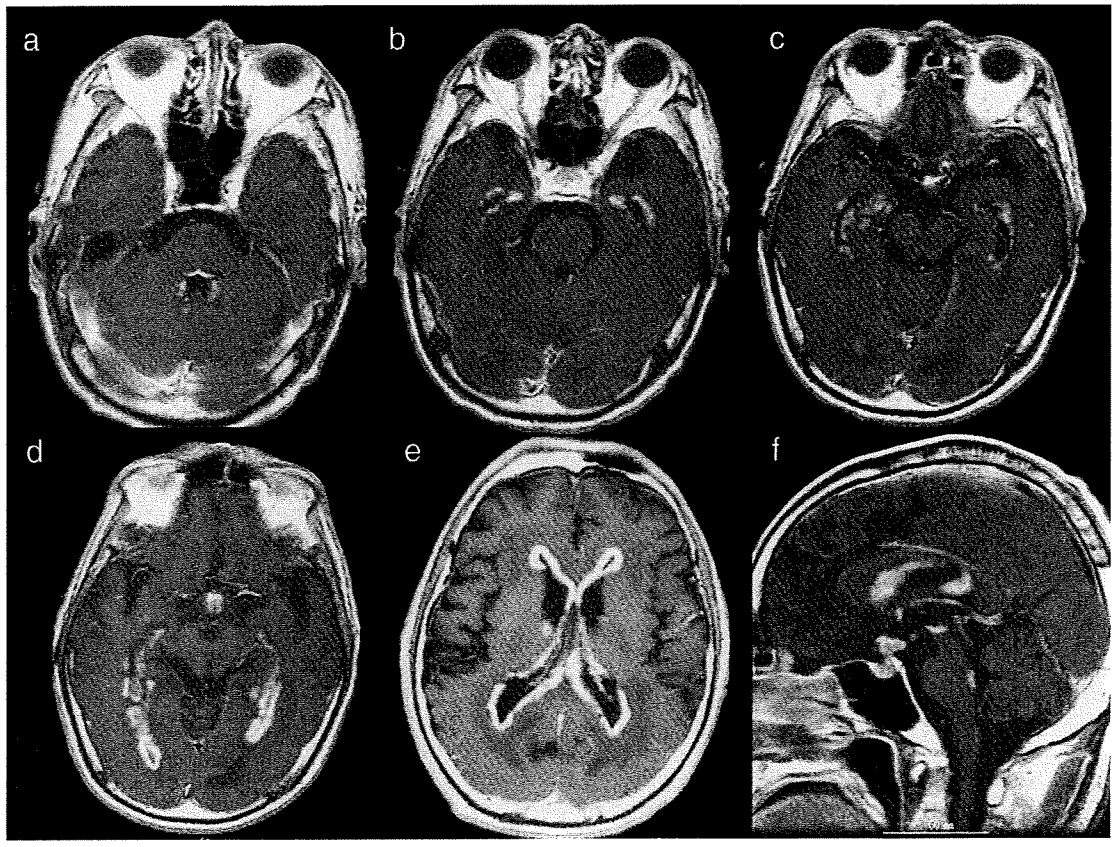

Fig. 2. Gadolinium-enhanced T1-weighted image disclosed abnormal enhancement around the lateral ventricle, third ventricle, fourth ventricle, and pituitary gland. Low intensity areas were also seen at the periventricular parenchyma, suggesting edema.

suggesting edema (Fig. 2). Cerebrospinal fluid (CSF) examination showed a cell count of 1/mm^3, total protein 150 mg/dl, glucose 56 mg/dl, sIL-2R 363 U/ml (normal range <85). Cytology of the CSF was negative. Biopsy of the left supraclavicular lymph nodes established a diagnosis of diffuse large B-cell lymphoma. However, repeated (six times) CSF examinations did not detect lymphoma cells. Although the symptoms and MRI findings improved with the intravenous administration of corticosteroid (hydrocortisone of 100 mg/day) and intralumbar methotrexate (15 mg/week) (Fig. 3), he died of multiple organ failure about 5 months after the onset.

At autopsy, swelling of the systemic lymph nodes, and masses at the left supraclavicular area, pancreas, abdominal aorta, and left adrenal gland were demonstrated. Ascites was also present. Microscopic examination disclosed that the lymphoma cells invaded the liver, pancreas, spleen, left adrenal gland, large bowel, and bone marrow.

The brain weight was 1430 g before fixation. Brain tissue samples were fixed postmortem with 10% formalin and embedded in paraffin. Ten-micrometer-thick sections from the right frontal lobe (the most anterior section), left head of the caudate nucleus, left amygdala, right subthalamic nucleus, right lateral geniculate body, right pulvinar nucleus, right occipital lobe, pons, medulla oblongata, and bilateral cerebellum were prepared. These sections were stained by hematoxylin-eosin (H&E) and Klüver-Barrera (KB) methods.

External examination disclosed fresh subdural and subarachnoid hemorrhages. A large thrombus was found in the superior sagittal sinus. Leptomeninges were unremarkable. On sections, fresh hemorrhages were seen in the left posterior lobe and left cerebellum. Microscopically, tumor cells were disseminated in the parenchyma adjacent to the bilateral anterior horn, bilateral inferior horn, and right posterior horn of the lateral ventricle, and the bottom of the third ventricle. The bilateral caudate nucleus, septum pellucidum, right thalamus, bilateral hippocampus, white matter of the right occipital lobe, and trunk of the corpus callosum were involved (Figs. 4, 5). Tumor cells were occasionally located in the Virchow-Robin space. Ependymal cells disappeared at the lesions where the tumor cells invaded (Fig. 5a). Tumor cells were also seen in the fourth ventricle, and in some parts of the dura and pia mater. The parenchymal lesions included necrotic foci and vascular proliferation. Tumor cells were not demonstrated in the choroid plexus within the sections. Immunophenotyping demonstrated that the infiltrating cells were CD20 (L26, mouse, monoclonal, 1:100, Dako) positive (Fig. 5b).

3. Discussion

We demonstrated periventricular involvement on MRI, and periventricular dissemination of lymphoma cells on postmortem study in a patient with systemic lymphoma. The enhancement with contrast medium is usually due to a breakdown of the blood-brain barrier (BBB). In our case, periventricular lesions included vascular proliferation probably associated with tumor neovascularity. Because the abnormal vessels had no effective BBB, the periventricular areas were distinctly enhanced by contrast medium.

Primary CNS lymphoma sometimes manifests as periventricular dissemination that damages the corpus callosum, periventricular white matter, thalamus, or basal ganglia [2]. Smirniotopoulos et al. stated that thick periventricular enhancement is seen in primary CNS lymphoma or high-grade astrocytoma, and thin (<2 mm, more often 1 mm) periventricular enhancement in infectious ependymitis [2]. In contrast, metastatic CNS lymphoma usually manifests as pachymeningeal or leptomeningeal infiltrates [1,2]. Parenchymal lesions, when present, typically result from secondary involvement of the leptomeninges [1] and rarely manifests as periventricular dissemination. In 1990, Nakasu et al. reported that there had been four cases showing periventricular involvement by metastatic CNS lymphoma on CT [3]. Since then, similar cases have not been reported. In the case reported by Dubois et al., the periventricular dissemination of lymphoma cells was confirmed at autopsy, however, the reason why tumors manifested as periventricular

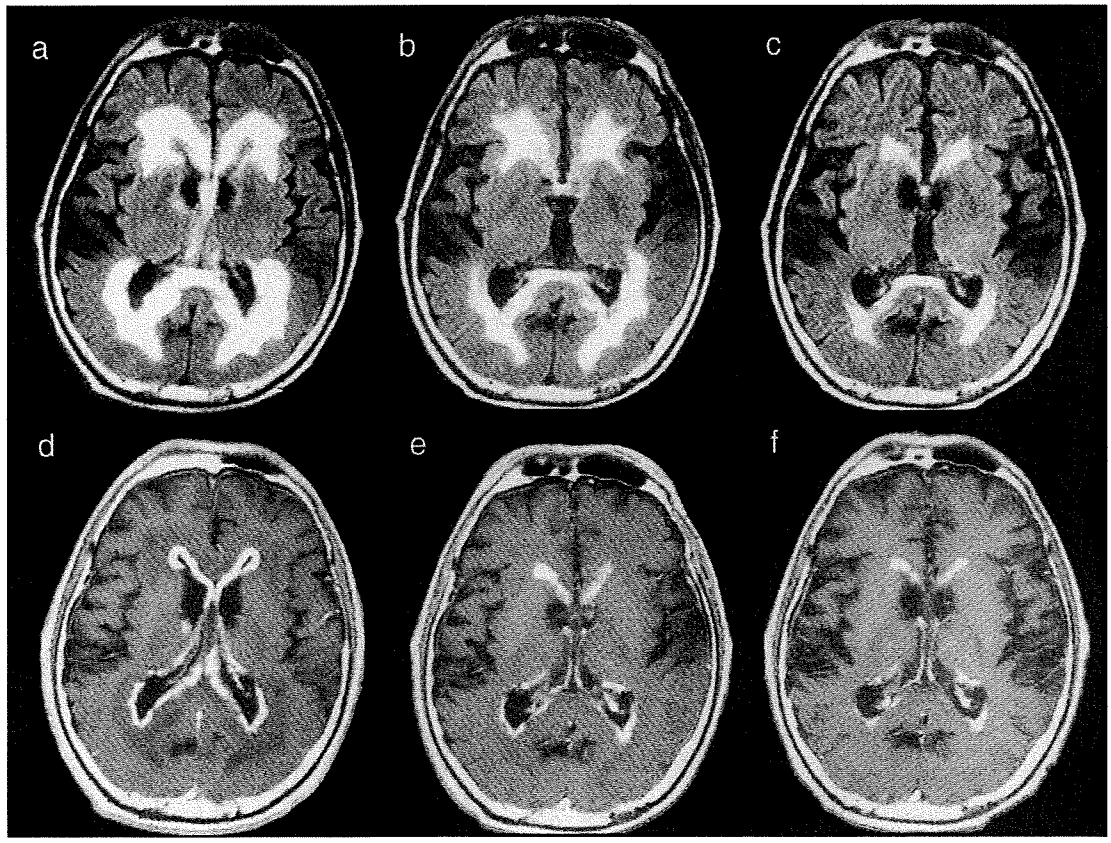

Fig. 3. Serial images (a, d: on admission, b, e: after 17 days of treatment, c, f: after 71 days of treatment) demonstrated improvement of the abnormal findings.

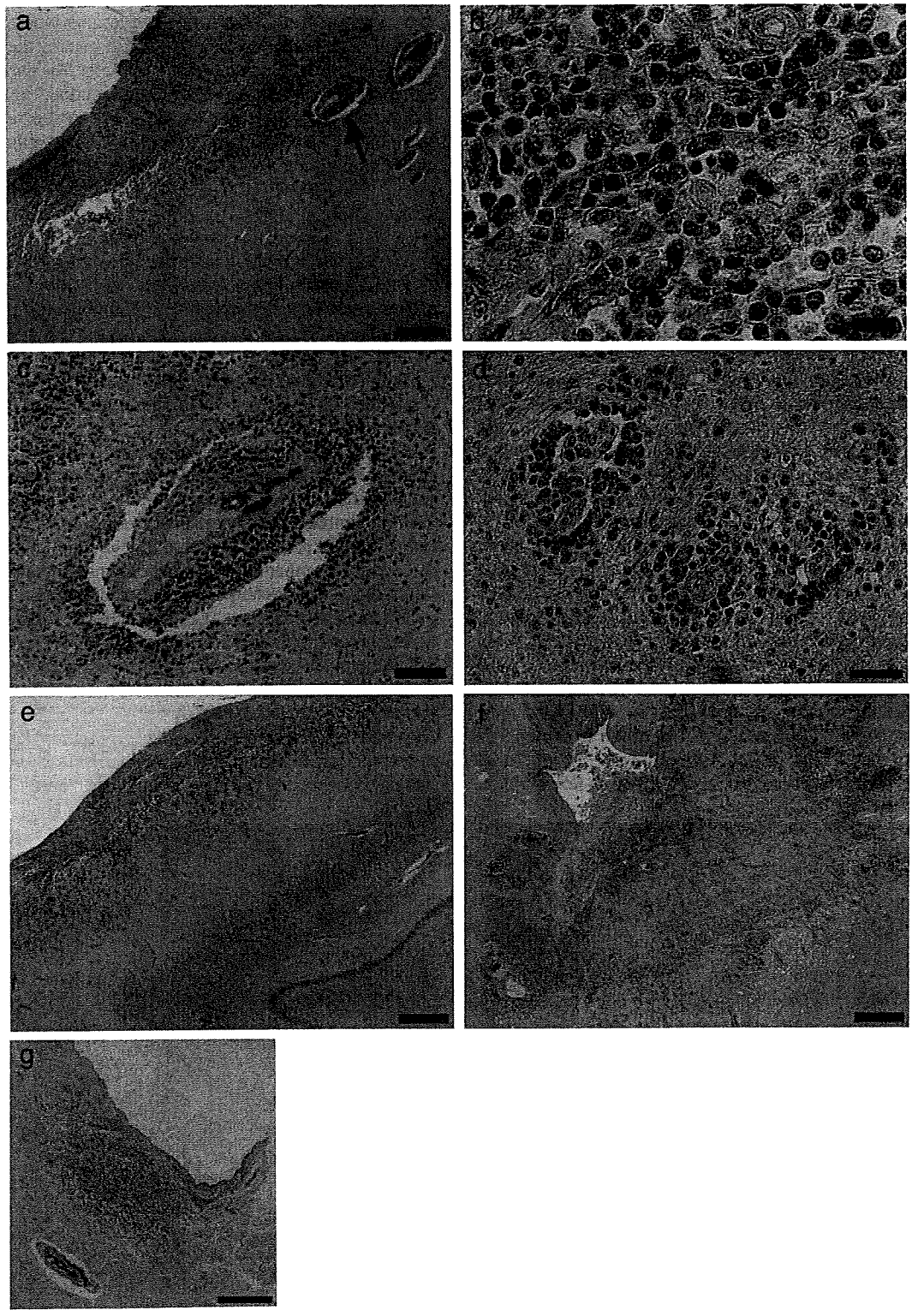

Fig. 4. Coronal section demonstrated infiltration of the tumor cells, necrosis, and vascular proliferation in the left head of the caudate nucleus (a). The vessel indicated with an arrow is shown in (c). Infiltrating cells were polymorphic, and the nucleolus was clearly observed (b). Tumor cells were also seen in the Virchow-Robin space (c). Vascular proliferation was seen, and each vessel was surrounded by tumor cells (d). Tumor cells were seen in the right Ammon's horn (e), white matter of the occipital lobe adjacent to the posterior horn of lateral ventricle (f), bottom of the third ventricle (g). Scale bar: a, e, f, g 500 μm, b 20 μm, c 100 μm, d 50 μm. a–g H&E stain.

dissemination was not described [4]. Apart from lymphoma, Vannier et al. reported three autopsy cases showing a pattern of periventricular dissemination of cerebral metastases from lung cancer. In their cases, CSF examination showed a moderately increased protein level, normal glucose, rare lymphocytes, and no malignant cells. Autopsy disclosed severe involvement of the periventricular area, and involvement of the choroid plexus was demonstrated in two of three cases. In the all cases, leptomeningeal involvement was minimal [5]. These CSF and autopsy findings were almost identical to those of our case, and suggested that the tumor cells had mainly invaded the ventricular system.

Why do tumors manifest as periventricular dissemination? Mcgeachie et al. proposed two mechanisms of periventricular dissemination in

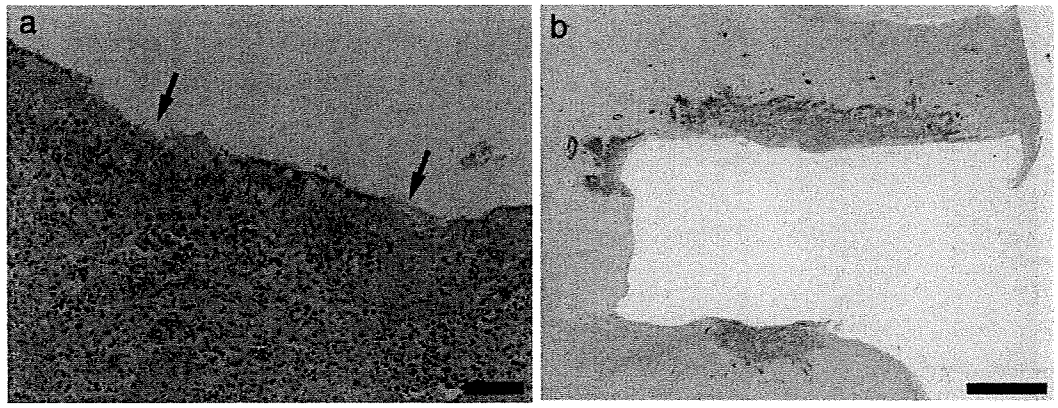

Fig. 5. Ependymal cells disappeared at the right thalamic lesions where the tumor cells invaded (a, arrow). Infiltrating cells of the trunk of the corpus callosum, body of the right caudate nucleus, and right thalamus were CD20 positive (b). Scale bar: a 100 μm, b 3 mm. a H&E stain.

the cases of glioma, glioblastoma, or melanoma. One is that tumors spread by infiltration over a long distance in the subependymal spaces as a diffuse sheet of advancing tumor cells. The other is that tumors invade the ventricular system and are then carried by the CSF and deposit in other parts of the ventricle where these cells invade the underlyng brain [6]. The "entrance" to the ventricular system was not described in the previous report, however, in our case, it may be the choroid plexus of the lateral ventricle because the most severe involvement was seen in the parenchyma around the lateral ventricle.

The choroid plexus consists of, from the inner side, many capillaries, loose connective tissue, and choroidal epithelium. Like the renal glomeruli, the capillaries have fenestrated endothelium through which solutes can pass [7]. This is one possible reason why the choroid plexus serves as the portal of entry into the CSF for hematogenously disseminated pathogens. Although we could not demonstrate lymphoma cells in the choroid plexus itself, the choroid plexus seen in the sections comprised only one part of the whole choroid plexus. The CSF might have carried the lymphoma cells from the lateral ventricle to the third and fourth ventricles, followed by periventricular dissemination. Regarding treatment, intra-CSF chemotherapy, if possible, may prefer intraventricular administration to intralumbar administration [8], especially in patients with periventricular involvement.

In conclusion, we reported an autopsy case of metastatic CNS lymphoma presenting with periventricular dissemination. Clinicians should consider not only primary CNS lymphoma but also metastatic CNS lymphoma, when periventricular lesions are seen on brain images.

Acknowledgement

This work was supported by a grant-in-aid for scientific research from the Ministry of Education, Culture, Sports, Science and Technology (14570957) and a research grant from the Zikei Institute of Psychiatry.

References

[1] Slone HW, Blake JJ, Shah R, Guttikonda S, Bourekas EC. CT and MRI findings of intracranial lymphoma. AJR Am J Roentgenol 2005;184:1679–85.
[2] Smirniotopoulos JG, Murphy FM, Rushing EJ, Rees JH, Schroeder JW. Patterns of contrast enhancement in the brain and meninges. Radiographics 2007;27:525–51.
[3] Nakasu Y, Nakasu S, Isozumi T, Handa J, Fujiyoshi K, Akiguchi I. Periventricular spread of malignant lymphoma: report of two cases. Nippon Geka Hokan 1990;59:323–9.
[4] Dubois PJ, Martinez AJ, Myerowitz RL, Rosenbaum AE. Case report: subependymal and leptomeningeal spread of systemic malignant lymphoma demonstrated by cranial computed tomography. J Comput Assist Tomogr 1978;2:218–21.
[5] Vannier A, Gray F, Gherardi R, Marsault C, Degos JD, Poirier J. Diffuse subependymal periventricular metastases. Report of three cases. Cancer 1986;58:2720–5.
[6] McGeachie RE, Gold LH, Latchaw RE. Periventricular spread of tumor demonstrated by computed tomography. Radiology 1977;125:407–10.
[7] Levine S. Choroid plexus: target for systemic disease and pathway to the brain. Lab Invest 1987;56:231–3.
[8] Gleissner B, Chamberlain M. Treatment of CNS dissemination in systemic lymphoma. J Neurooncol 2007;84:107–17.

Acta Neuropathol
DOI 10.1007/s00401-009-0612-2

CONSENSUS PAPER

Nomenclature and nosology for neuropathologic subtypes of frontotemporal lobar degeneration: an update

Ian R. A. Mackenzie · Manuela Neumann · Eileen H. Bigio · Nigel J. Cairns · Irina Alafuzoff · Jillian Kril · Gabor G. Kovacs · Bernardino Ghetti · Glenda Halliday · Ida E. Holm · Paul G. Ince · Wouter Kamphorst · Tamas Revesz · Annemieke J. M. Rozemuller · Samir Kumar-Singh · Haruhiko Akiyama · Atik Baborie · Salvatore Spina · Dennis W. Dickson · John Q. Trojanowski · David M. A. Mann

Received: 9 November 2009 / Accepted: 10 November 2009

One year ago, in this journal, we published a recommended nomenclature for the neuropathologic subtypes of frontotemporal lobar degeneration (FTLD) [7]. A major impetus behind this was to resolve the confusion that had arisen around the use of the term "FTLD with ubiquitinated inclusions" (FTLD-U), following the discovery that the molecular pathology of these cases was heterogeneous, with most, but not all, being characterized by pathological TDP-43 [6, 11]. In addition, a system of nosology was introduced that grouped the FTLD subtypes into broad categories, based on the molecular defect that is most characteristic, according to current evidence. This system provided a concise and consistent terminology that has now been widely adopted in the literature. Another anticipated advantage was the ability to readily accommodate new discoveries. At the time, we did not anticipate how quickly this attribute would be put to use.

Although most FTLDs are characterized by cellular inclusion bodies composed of either tau (FTLD-tau) or TDP-43 (FTLD-TDP), approximately 10–15% of cases

I. R. A. Mackenzie (✉)
Department of Pathology and Laboratory Medicine,
Vancouver General Hospital and University of British Columbia,
855 West 12th Ave., Vancouver, BC V5Z 1M9, Canada
e-mail: ian.mackenzie@vch.ca

M. Neumann
Institute of Neuropathology, University Hospital of Zurich,
Zurich, Switzerland

E. H. Bigio
Department of Pathology, Northwestern University Feinberg
School of Medicine, Chicago, IL, USA

N. J. Cairns
Department of Pathology and Immunology,
Washington University School of Medicine, St. Louis, MO, USA

I. Alafuzoff
Department of Genetics and Pathology,
Uppsala University, Uppsala, Sweden

J. Kril
Department of Pathology, The University of Sydney,
Sydney, NSW, Australia

G. G. Kovacs
Institute of Neurology, Medical University of Vienna,
Vienna, Austria

B. Ghetti · S. Spina
Department of Pathology and Laboratory Medicine,
Indiana University School of Medicine, Indianapolis, IN, USA

G. Halliday
Prince of Wales Medical Research Institute,
University of New South Wales, Sydney, NSW, Australia

I. E. Holm
Laboratory for Experimental Neuropathology,
Danish Neuroscience Center, Aarhus University Hospital,
Aarhus, Denmark

P. G. Ince
Department of Neuroscience, University of Sheffield Medical
School, Sheffield, UK

W. Kamphorst · A. J. M. Rozemuller
Department of Pathology, Vrije University Medical Centre,
Amsterdam, The Netherlands

T. Revesz
Department of Molecular Neuroscience, UCL Institute
of Neurology, Queen Square Brain Bank, Queen Square,
London, UK

S. Kumar-Singh
VIB-Department of Molecular Genetics, University of Antwerp,
Antwerp, Belgium

Published online: 19 November 2009

remain, that include a number of uncommon FTLD subtypes, in which the pathologic protein is unknown. Recently, two studies identified mutations in the gene encoding the *fused in sarcoma* (FUS) protein (also known as *translocated in liposarcoma*, TLS), as the cause of familial amyotrophic lateral sclerosis (ALS) type 6 [5, 14]. The recognized clinical, genetic and pathological overlap between ALS and FTD, and the high degree of functional homology between FUS and TDP-43, prompted a number of subsequent studies that demonstrated that the inclusions of several of the tau/TDP-43-negative FTLDs are immunoreactive (ir) for FUS [8–10]. One such group are those cases with TDP-43-negative FTLD-U pathology, originally referred to as atypical FTLD-U (aFTLD-U) [6, 11]. According to the previous nomenclature recommendations, the neuropathology of these cases was designated as FTLD-UPS because the inclusions were only detectable with immunohistochemistry against proteins of the ubiquitin proteasome system (UPS) [7]. However, based on the discovery that all the ubiquitin-positive pathology in these cases is immunoreactive for FUS, we now recommend that they should be reclassified as FTLD-FUS [9]. In addition, the characteristic neuronal cytoplasmic inclusions of basophilic inclusions body disease (BIBD), previously of unknown biochemical composition, have also been shown to be consistently FUS-ir [8]. Perhaps most surprising has been the identification of abundant FUS-positive pathology in cases of neuronal intermediate filament inclusion disease (NIFID) [10]. The diagnostic criterion for NIFID is the presence of neuronal inclusions that are negative for tau, α-synuclein and TDP-43 but immunoreactive for class IV intermediate filaments (IF) [1] and therefore the term FTLD-IF was designated in the previous nomenclature recommendations [7]. However, the finding that only a minority of the inclusions in NIFID are IF-ir, the absence of any identifiable genetic or molecular abnormality of IF in these cases and the recognition that immunohistochemistry for IF is not specific for this condition, is consistent with the possibility that another protein may be more central to the pathogenesis. The recent demonstration that a much larger proportion of the inclusions in NIFID are FUS-ir, that all the cells with IF-ir inclusions also contain pathological FUS, and that there are widespread FUS-ir glial inclusions, suggests that the abnormal accumulation of FUS may be more fundamental in the disease process and that IF pathology probably develops as a secondary process [10].

Taking these studies together, we now recommend that aFTLD-U, BIBD and NIFID should be grouped together under the designation of FTLD-FUS (Table 1). It is important to recognize, however, that this does not imply that a defect in FUS metabolism is known to be causal in any of these conditions. Rather, it simply indicates that they share FUS accumulation as the most prominent molecular pathology. Whether or not this indicates that aFTLD-U, BIBD and NIFID are actually all part of a continuous spectrum of disease must await detailed comparative clinicopathological studies of larger numbers of cases. Nonetheless, the presence of FUS pathology sets these cases apart and should aid in their neuropathological diagnosis and classification.

Although it now appears that most, if not all, cases of sporadic FTLD-UPS (i.e. aFTLD-U) have FUS-immunoreactive pathology [9], the designation FTLD-UPS remains appropriate for at least one condition: familial FTD linked to chromosome 3 (FTD-3), caused by mutations in the *CHMP2B* gene. In addition to being negative for tau and TDP-43 [2], a recent study has shown that the ubiquitin/p62-immunoreactive neuronal inclusions in these cases do not label with antibodies against FUS [3]. Although these inclusions may eventually be discovered to contain a single major pathologic protein, it is also possible they have more heterogeneous composition that results from a primary defect of endosomal function [13]. Until this is determined, FTLD-UPS remains an appropriate designation for the neuropathology of FTD-3 and possibly for some FUS-negative sporadic cases.

With these recent advances, virtually all cases of FTLD can now be assigned to one of the three major molecular subgroups (FTLD-tau, FTLD-TDP or FTLD-FUS). This classification does not presuppose a primary role of the signature protein in pathogenesis (although in FTLD-tau and FTLD-TDP there is growing evidence to support this), but provides a logical way of grouping neuropathologic subtypes that is likely to have relevance regarding common disease mechanisms, diagnostic tests and possibly treatments. The specific role of the pathologic proteins and their relationship to causal gene defects is crucial information

H. Akiyama
Tokyo Institute of Psychiatry, Tokyo, Japan

A. Baborie
Department of Neuropathology, The Walton Centre for Neurology and Neurosurgery, Liverpool, UK

D. W. Dickson
Department of Neuropathology Laboratory, Mayo Clinic College of Medicine, Jacksonville, FL, USA

J. Q. Trojanowski
Department of Pathology and Laboratory Medicine, University of Pennsylvania School of Medicine, Philadelphia, PA, USA

D. M. A. Mann
Clinical Neuroscience Research Group, Greater Manchester Neurosciences Centre, University of Manchester, Salford, UK

Table 1 Updated nomenclature for neuropathologic subtypes of frontotemporal lobar degeneration

2009 recommendation		2010 recommendation		Associated genes
Major molecular class	Recognized subtypes[a]	Major molecular class	Recognized subtypes[a]	
FTLD-tau	PiD	FTLD-tau	PiD	*MAPT*
	CBD		CBD	
	PSP		PSP	
	AGD		AGD	
	MSTD		MSTD	
	NFT-dementia		NFT-dementia	
	WMT-GGI		WMT-GGI	
	Unclassifiable		Unclassifiable	
FTLD-TDP	Types 1–4	FTLD-TDP	Types 1–4	*GRN*
	Unclassifiable		Unclassifiable	*VCP*
				9p
				(TARDBP)[b]
FTLD-UPS	**FTD-3**	**FTLD-UPS**	**FTD-3**	*CHMP2B*
	aFTLD-U			
FTLD-IF	**NIFID**	**FTLD-FUS**	**aFTLD-U**	*(FUS)*[c]
BIBD			**NIFID**	
			BIBD	
FTLD-ni		FTLD-ni		

Entries in bold indicate major revisions

aFTLD-U, atypical frontotemporal lobar degeneration with ubiquitinated inclusions; AGD, argyrophilic grain disease; BIBD, basophilic inclusion body disease; CBD, corticobasal degeneration; CHMP2B, charged multivescicular body protein 2B; FTD-3, frontotemporal dementia linked to chromosome 3; FTLD, frontotemporal lobar degeneration; FUS, fused in sarcoma; *GRN*, progranulin gene; IF, intermediate filaments; MAPT, microtubule associated protein tau; MSTD, multiple system tauopathy with dementia; NFT-dementia, neurofibrillary tangle predominant dementia; ni, no inclusions; NIFID, neuronal intermediate filament inclusion disease; PiD, Pick's disease; PSP, progressive supranuclear palsy; TARDBP, transactive response DNA binding protein; TDP, TDP-43; UPS, ubiquitin proteasome system; VCP, valosin containing protein; WMT-GGI, white matter tauopathy with globular glial inclusions; 9p, genetic locus on chromosome 9p linked to familial amyotrophic lateral sclerosis and frontotemporal dementia

[a] Indicates the characteristic pattern of pathology, not the clinical syndrome. Note that FTDP-17 is not listed as a pathological subtype because cases with different *MAPT* mutations do not have a consistent pattern of pathology. These cases would all be FTLD-tau, but further subtyping would vary

[b] Rare case reports of patients with clinical FTD and TDP-43 pathology associated with *TARDBP* genetic variants [4]

[c] One patient reported with a *FUS* mutation and FTD/ALS clinical phenotype but no description of pathology [12]

that requires further neuropathological and experimental investigations.

References

1. Cairns NJ, Uryu K, Bigio E et al (2004) α-Internexin in neuronal intermediate filament inclusion disease and other neurodegenerative diseases. Acta Neuropathol 108:213–223. doi:10.1007/s00401-004-0882-7
2. Holm IE, Englund E, Mackenzie IRA, Johannsen P, Isaacs A (2007) A reassessment of the neuropathology of frontotemporal dementia linked to chromosome 3 (FTD-3). J Neuropathol Exp Neurol 66:884–891. doi:10.1097/nen.0b013e3181567f02
3. Holm IE, Isaacs A, Mackenzie IRA (2009) Absence of FUS-immunoreactive pathology in frontotemporal dementia linked to chromosome 3 (FTD-3) caused by mutation in the *CHMP2B* gene. Acta Neuropathol 118:719–720. doi:10.1007/s00401-009-0593-1
4. Kovacs GG, Murrell JR, Horvath S et al (2009) TARDBP variation associated with frontotemporal dementia, supranuclear gaze palsy and chorea. Mov Disord 24:1843–1847. doi:10.1002/mds.22697
5. Kwiatkowski TJ, Bosco DA, LeClerc AL et al (2009) Mutations in the FUS/TLS gene on chromosome 16 cause familial amyotrophic lateral sclerosis. Science 323:1205–1208. doi:10.1126/science.1166066
6. Mackenzie IRA, Foti D, Woulfe J, Hurwitz TA (2008) Atypical frontotemporal lobar degeneration with ubiquitin-positive, TDP-43-*negative* neuronal inclusions. Brain 131:1282–1293. doi:10.1093/brain/awn061
7. Mackenzie IR, Neumann M, Bigio EH et al (2009) Nomenclature for neuropathologic subtypes of frontotemporal lobar degeneration: consensus recommendations. Acta Neuropathol 117:15–18. doi:10.1007/s00401-008-0460-5

8. Munoz DG, Neumann M, Kusaka H et al (2009) FUS pathology in basophilic inclusion body disease. Acta Neuropathol 118:617–627. doi:10.1007/s00401-009-0598-9
9. Neumann M, Rademakers R, Roeber S, Baker M, Kretzschmar HA, Mackenzie IRA (2009) Frontotemporal lobar degeneration with FUS pathology. Brain 132:2922–2931. doi:10.1093/brain/awp214
10. Neumann M, Roeber S, Kretzschmar HA, Rademakers R, Baker M, Mackenzie IRA (2009) Abundant FUS pathology in neuronal intermediate filament inclusion disease. Acta Neuropathol 118:605–616. doi:10.1007/s00401-009-0581-5
11. Roeber S, Mackenzie IR, Kretzschmar HA, Neumann M (2008) TDP-43-negative FTLD-U is a significant new clinico-pathological subtype of FTLD. Acta Neuropathol 116:147–157. doi:10.1007/s00401-008-0395-x
12. Ticozzi N, Silani V, LeClerc AL et al (2009) Analysis of *FUS* gene mutation in familial amyotrophic lateral sclerosis within an Italian cohort. Neurology 73:1180–1185. doi:10.1212/WNL.0b013e3181bbff05
13. Urwin H, Ghazi-Noori S, Collinge J, Isaacs A (2009) The role of CHMP2B in frontotemporal dementia. Biochem Soc Trans 37:208–212. doi:10.1042/BST0370208
14. Vance C, Rogelj B, Hortobagyi T et al (2009) Mutations in FUS, an RNA processing protein, cause familial amyotrophic lateral sclerosis type 6. Science 323:1208–1211. doi:10.1126/science.1165942

NEUROPATHOLOGY

doi:10.1111/j.1440-1789.2009.01089.x

Neuropathology 2010

Symposium: Advances in amyotrophic lateral sclerosis research

Phosphorylated and cleaved TDP-43 in ALS, FTLD and other neurodegenerative disorders and in cellular models of TDP-43 proteinopathy

Tetsuaki Arai,[1] Masato Hasegawa,[2] Takashi Nonoka,[2] Fuyuki Kametani,[2] Makiko Yamashita,[2] Masato Hosokawa,[1] Kazuhiro Niizato,[1,3] Kuniaki Tsuchiya,[1,4] Zen Kobayashi,[1,5] Kenji Ikeda,[6] Mari Yoshida,[7] Mitsumoto Onaya,[8] Hiroshige Fujishiro[9] and Haruhiko Akiyama[1]

Departments of [1]Psychogeriatrics and [2]Molecular Neurobiology, Tokyo Institute of Psychiatry, Tokyo Metropolitan Organization for Medical Research, Departments of [3]Psychiatry and [4]Laboratory Medicine and Pathology, Tokyo Metropolitan Matsuzawa Hospital, [5]Department of Neurology and Neurological Science, Graduate School, Tokyo Medical and Dental University, Tokyo, [6]Zikei Hospital, Zikei Institute of Psychiatry, Okayama, [7]Department of Neuropathology, Institute for Medical Science of Aging, Aichi Medical University, Aichi, [8]Department of Neuropsychiatry, National Shimofusa Mental Hospital, Chiba, [9]Juntendo Tokyo Koto Geriatric Medical Center, Juntendo University School of Medicine, Tokyo, Japan

Transactivation response (TAR) DNA-binding protein of Mr 43 kDa (TDP-43) is a major component of the tau-negative and ubiquitin-positive inclusions that characterize amyotrophic lateral sclerosis (ALS) and frontotemporal lobar degeneration which is now referred to as FTLD-TDP. Concurrent TDP-43 pathology has been reported in a variety of other neurodegenerative disorders such as Alzheimer's disease, forming a group of TDP-43 proteinopathy. Accumulated TDP-43 is characterized by phosphorylation and fragmentation. There is a close relationship between the pathological subtypes of FTLD-TDP and the immunoblot pattern of the C-terminal fragments of phosphorylated TDP-43. These results suggest that proteolytic processing of accumulated TDP-43 may play an important role for the pathological process. In cultured cells, transfected C-terminal fragments of TDP-43 are more prone to form aggregates than full-length TDP-43. Transfecting the C-terminal fragment of TDP-43 harboring pathogenic mutations of TDP-43 gene identified in familial and sporadic ALS cases into cells enhanced the aggregate formation. Furthermore, we found that methylene blue and dimebon inhibit aggregation of TDP-43 in these cellular models. Understanding the mechanism of phosphorylation and truncation of TDP-43 and aggregate formation may be crucial for clarifying the pathogenesis of TDP-43 proteinopathy and for developing useful therapeutics.

Key words: α-synuclein, fragment, inclusion, phosphorylation, tau.

INTRODUCTION

Transactivation response (TAR) DNA-binding protein of Mr 43 kDa (TDP-43) is a major component of the tau-negative and ubiquitin-positive inclusions that characterize amyotrophic lateral sclerosis (ALS) and the most common pathological subtype of frontotemporal lobar degeneration (FTLD-U), which is now referred to as FTLD-TDP.[1-7] Several genes and chromosomal loci, including the progranulin gene (*PGRN*),[8,9] valosin-containing protein gene (*VCP*)[10] and an unidentified gene at chromosome 9p,[11,12] have been reported to be associated with familial forms of FTLD-TDP. Recent findings of various missense mutations of TDP-43 gene (*TARDBP*) in familial and sporadic ALS cases prove the essential role of abnormal TDP-43 in neurodegeneration.[13-17] These disorders are now collectively referred to as TDP-43 proteinopathy.[1-4]

Correspondence: Haruhiko Akiyama, MD, PhD, Departments of Psychogeriatrics, Tokyo Institute of Psychiatry, Tokyo Metropolitan Organization for Medical Research, 2-1-8 Kamikitazawa, Setagaya-ku, Tokyo 156-8585, Japan. Email: akiyama@prit.go.jp

Received 29 October 2009; revised 14 November 2009 and accepted 15 November 2009.